

Fluctuation Suppression during the ECH Induced Potential Formation in the Tandem Mirror GAMMA 10

M. Yoshikawa 1), Y. Miyata 1), M. Mizuguchi 1), Y. Oono 1), F. Yaguchi 1), M. Ichimura 1), T. Imai 1), T. Kariya 1), I. Katanuma 1), Y. Nakashima 1), H. Hojo 1), R. Minami 1), and Y. Yamaguchi 1)

1) Plasma Research Center, University of Tsukuba, Tsukuba, Ibaraki 305-8577, Japan

E-mail contact of main author: yosikawa@prc.tsukuba.ac.jp

Abstract. The suppression of the potential fluctuation was clearly observed during the radial potential profile change and positive electric fields driven by electron cyclotron heating. The particle flux evaluated from the phase difference between the potential and density fluctuations measured by a gold neutral beam probe showed the radial outward flux and its correlation with the decrease in the stored energy. When flux is suppressed by the potential formation, the plasma stored energy increases quickly. These indicate that the observed fluctuations are the one of the source of the anomalous radial transport and the radial profile of the potential is one of the keys to control plasma transport.

1. Introduction

In the tandem mirror GAMMA 10, an electrostatic potential for improving an axial confinement is created by applying electron cyclotron resonance heating (ECH) in the end mirrors (plug/barrier cells) [1-6]. Two types of instabilities, a rotationally driven mode with the lowest azimuthal mode number and a drift-wave mode with high mode numbers, are observed during the existence of confining potentials. The rotational mode is driven by $E \times B$ rotation at the lowest azimuthal mode number $m = 1$ in tandem mirrors. The higher modes with $m \geq 2$ will be stabilized by finite Larmor radius effects. On the other hand, the drift-wave mode arises due to the existence of density and temperature gradients. The radial electric field E due to the potential causes an $E \times B$ plasma rotation in the direction of the ion diamagnetic drift, which may enhance instabilities such as rotational flute modes, and degrade radial confinement. While present studies show that the suppression of low frequency fluctuations on the density and the potential during the formation of axial confinement potential by plug-ECH (P-ECH) [1-3, 4-6]. The former works by Sanuki [7] and Chaudhry et al. [8] discussed the effects of ambipolar potential on the stability of drift waves. The stability is considered to be due to the ion Landau damping caused from the velocity shear effect of the $E \times B$ rotation [9-12]. The density fluctuation is observed using microwaves, such as interferometer, reflectometry and Fraunhofer diffraction method, and electrostatic probes [1-3,5,6]. In GAMMA 10, there is a good potential measurement system that is a gold neutral beam probe system (GNBP) [4,13]. We can observe the density and potential fluctuations when the axial confinement potential is formed during the application of P-ECH in a single plasma shot. In the former experiments, the potential and potential fluctuation were obtained at only one plasma radial position. We tried to obtain the two radial positions' potentials and their fluctuations in a single plasma shot with applying the rectangular wave form at the vertical beam deflector electrode. It is successfully obtained the potential and its fluctuations of two radial positions. We obtained the radial electric field profile, and observed the suppressions of density and potential fluctuations by the potential formation during P-ECH by using the GNBP. It is possible to study more detail about the suppression mechanisms of drift-type fluctuation during the formation of confinement potential produced

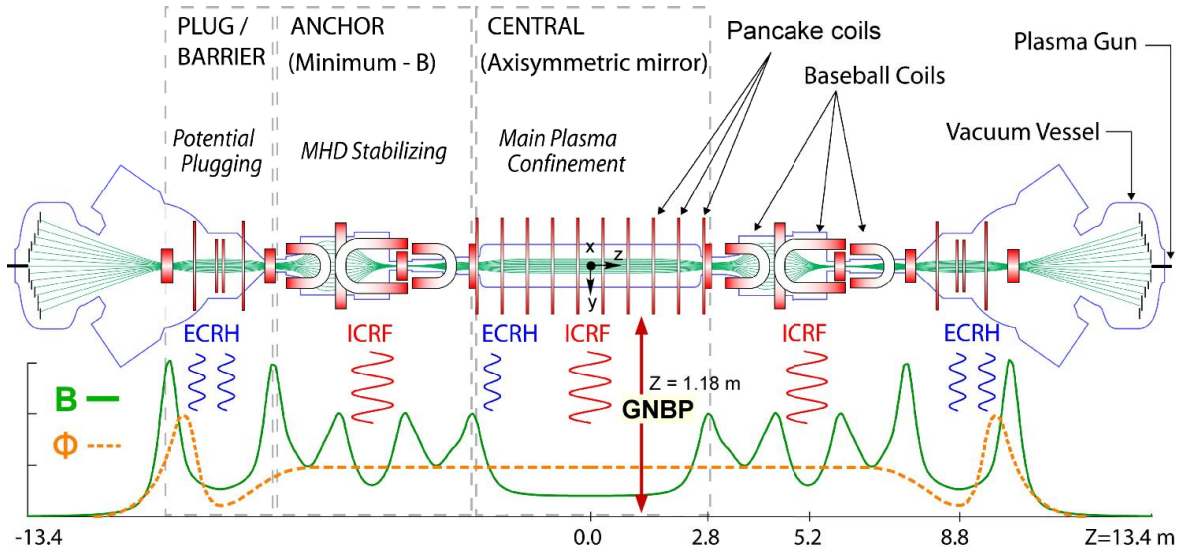


FIG. 1. The schematic of the tandem mirror GAMMA 10.

by P-ECH.

In this paper, we show the relationships between the suppression of potential fluctuation of drift-type mode and the potential and electric field radial profiles. The particle flux related value is obtained by the phase differences between the electron density fluctuation and the potential fluctuation. These indicate that the observed fluctuations are the one of the source of the anomalous radial transport and the radial profile of the potential is one of the keys to control plasma transport.

2. Experimental Apparatus

2.1 Tandem mirror GAMMA 10

GAMMA 10 is an effectively axisymmetrized minimum-B anchored tandem mirror with thermal barrier at both end-mirrors (Fig. 1). Detail of GAMMA 10 is shown in elsewhere [1-6]. The x-axis and the y-axis are perpendicular to the magnetic field in the horizontal and vertical directions, respectively. The z-axis is parallel to the magnetic field. In the tandem mirror GAMMA 10, the lengths of central, anchor and plug/barrier cells are 6.0 m, 4.8 m and 2.5 m, respectively. Magnetic field strength at the mid-plane of the central cell is 0.41 T in the standard operation and mirror ratio is 5. The anchor cells are located at both sides of the central cell and consist of minimum-B mirror field which is produced by a base ball coil. The magnetic field strength is 0.61 T at the mid-plane of the anchor cell and mirror ratio is 3. The plug/barrier cells are located at both ends of GAMMA 10, where the electron confinement potentials and ion confinement potentials are produced by the application of B/P-ECH. The plasma is created by plasma guns, and heated and sustained using ion cyclotron range of frequency (ICRF) heating systems. There are three types of oscillators named RF1, RF2 and RF3. The waves excited with RF1 and RF2 systems take on the plasma production and ion heating in the central cell, respectively. The difference between the central potential (Φ_c) and the plug potential (Φ_p) is the ion confining potential (ϕ_p). The difference between the central potential (Φ_c) and the barrier potential (Φ_b) is the thermal barrier potential (ϕ_b). The typical electron density, electron and ion temperatures are about $2 \times 10^{12} \text{ cm}^{-3}$, 0.1 keV and 5 keV, respectively. The typical central, barrier and plug potentials are about 500 V, 0 V, and 1.7 kV with P-ECH of 250 kW power, respectively.

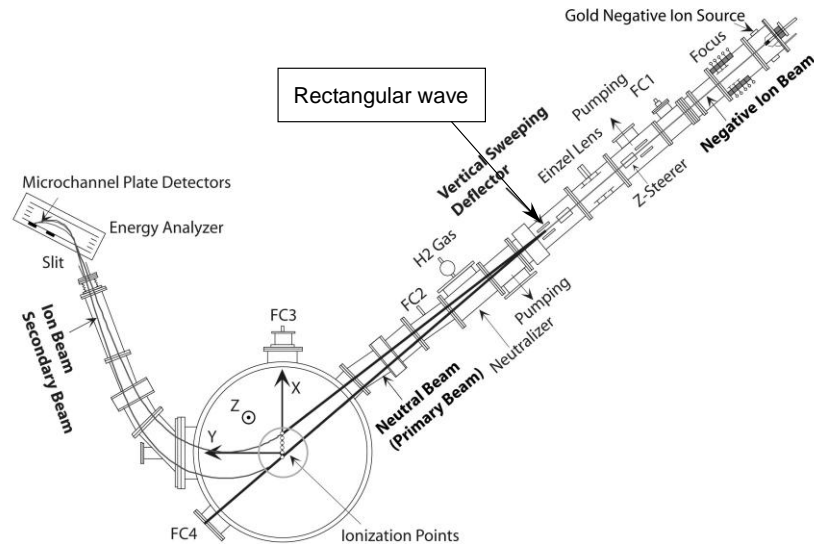


FIG. 2. GNBP system in GAMMA 10. We applied rectangular wave to the vertical deflector electrode.

2. 2. Gold Neutral Beam Probe

We use the heavy ion beam probe for potential measurement of core plasma at central cell in GAMMA 10. We measured the potential and its fluctuation by using GNBP in the central cell ($z = 1.18$ m) (Fig. 2) [9]. In the case of a vertically directed beam sweep for radial potential profile observations in a single plasma shot, ionization points move in the vertical direction due to the incident angle changes. The features of GNBP are using the neutral primary beam and the negative gold ion by Cs sputtering [4]. The energy and the incident angle of the primary beam passing the plasma center are about 12 keV and 40 degrees, respectively. Typical primary beam current is $2 \mu\text{A}$, which is measured by using the Faraday Cup. The GNBP has two incident angle electrostatic deflectors of the vertical and the horizontal directions. A parallel plate type electrostatic energy analyzer with the incident angle of 45 degrees is installed on the x-y plane. In the analyzer, the micro-channel plate detector of 32 anodes which is mounted along y direction is utilized for the beam detector.

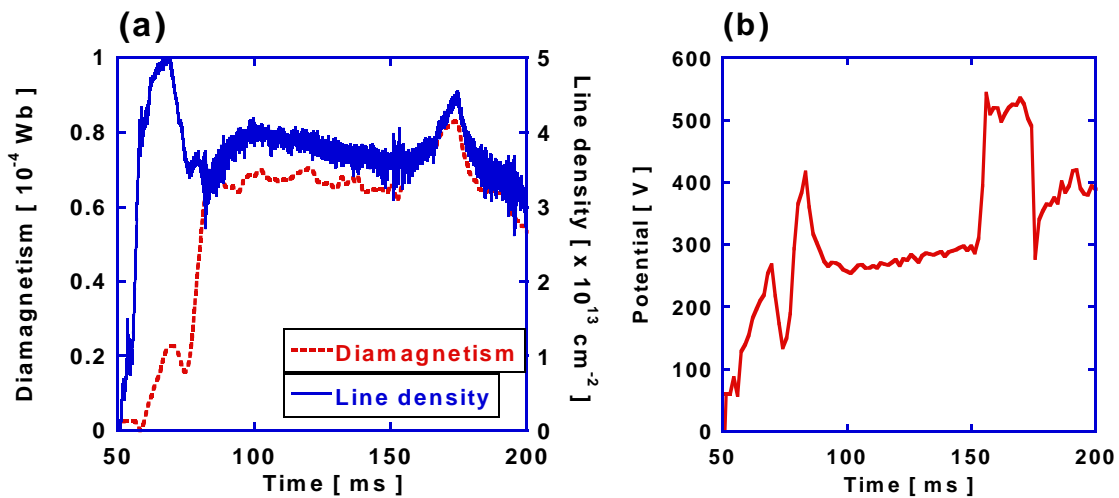


FIG. 3. (a) shows temporal behaviors of diamagnetism and electron line density and (b) shows the potential.

The detected positive secondary beam is derived from the neutral primary beam ionized at the ionization position. The electron-impact ionization process is dominant in a case of the ionization of the primary beam. The secondary beam current depends on the electron distribution function at the ionization position. The density fluctuation is obtained from the perturbation of the detected beam intensity, and the potential fluctuation is obtained from the perturbation of the plasma potential. It is possible to measure the potential, density fluctuations and their phase difference at the arbitrary point simultaneously by GNPB. GNPB can measure the radial potential profile from $R \sim 0$ cm to $R \sim 14$ cm in the error of ± 10 V. The path integral effect is low in the density and potential fluctuations measured in the density range and low fluctuation levels of GAMMA10 experiment [4].

3. Fluctuation Measurements

The radial potential and electric field profiles have been measured by applying the rectangular wave on the deflector electrodes of the GNPB system in order to measure the plasma

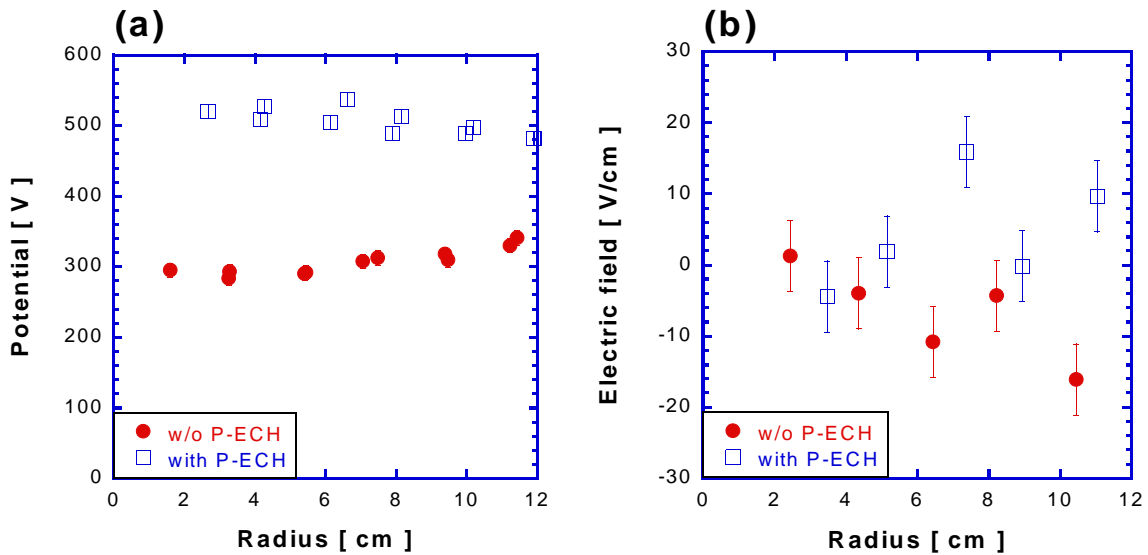


FIG. 4. (a) and (b) show the radial profiles of potential and electric field, without (closed circle) and with P-ECH (open square), respectively.

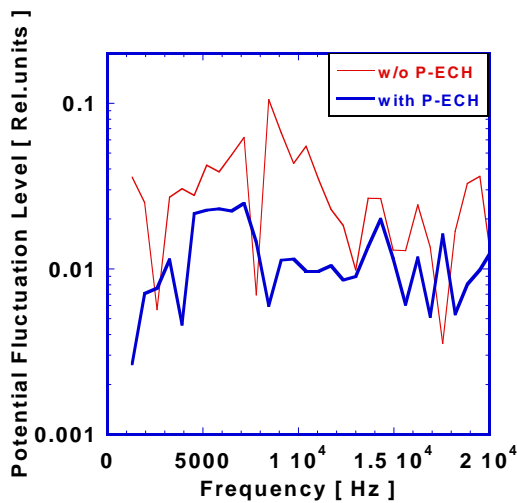


FIG. 5. The potential fluctuation spectra at $R \sim 5$ cm.

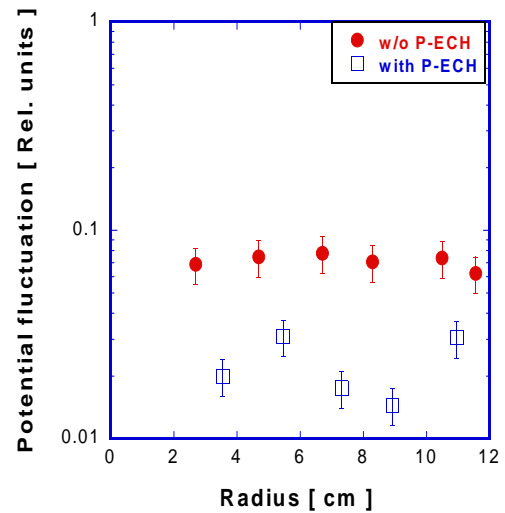


FIG. 6. The radial profile of potential fluctuation peaks at a frequency from 8 kHz to 12 kHz.

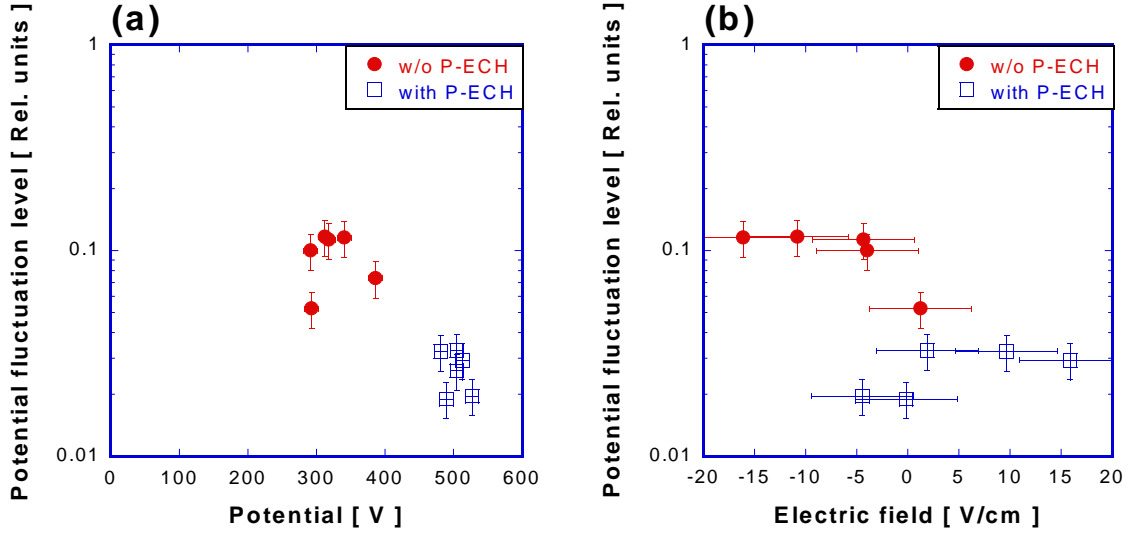


FIG. 7. (a) and (b) show the relationship between the potential and electric field strength and the potential fluctuations are shown, respectively.

potentials at two positions in a single plasma shot. The plasma was produced in the duration from 50 to 250 ms. The B-ECH and P-ECH were applied from 155 to 200 ms and 155 to 175 ms, respectively. The temporal evolution of the potential was measured by GNPB with P-ECH power of 250 kW. In these experiments, we concentrated to the core plasma region ($R < 12$ cm). Figure 3(a) shows temporal evolutions of diamagnetism (dotted line) and electron line density (solid line) and Fig. 3(b) shows that of the potential. The central potential increases quickly during the P-ECH period. Potential and electric field radial profiles were observed without and with P-ECH. In Fig. 4(a) and 4(b), we show the radial potential and electric field profiles, respectively. In those figures, closed circles and open squares show them without and with P-ECH, respectively. Before application of P-ECH, the radial potential profile had a profile in which the plasma center ($R \sim 0$ cm) had a lower potential than that at $R \sim 12$ cm. With the application of P-ECH, however, the radial potential profile had a higher potential at the plasma center ($R \sim 0$ cm) than that at $R \sim 12$ cm. In Fig. 5, the potential fluctuation spectra at $R \sim 5$ cm are shown. Thin line and bold line represent the potential fluctuation spectra without and with P-ECH, respectively. The potential fluctuation with frequency of about 10 kHz was observed and it corresponds to the diamagnetic drift-type fluctuations. Figure 6 shows the radial profile of potential fluctuation peaks in the frequency range from 8 kHz to 12 kHz. In this figure, the closed circles and the open squares show the potential fluctuation peaks without and with P-ECH periods, respectively. Potential fluctuation suppression with the application of P-ECH was clearly observed at each radial position. In Fig. 7(a) and 7(b), the relationship between the potential and electric field strength and the potential fluctuations are shown, respectively. The closed circles and the open squares show the potential fluctuation peaks without and with P-ECH periods, respectively. The potential fluctuation levels are smaller in the case of larger potential formation. Moreover, the potential fluctuations at the negative electric field region are larger than those at the positive electric fields region. Then the drift-type fluctuations are suppressed by the potential formation and positive electric field formation on the central cell. Considering the drift type fluctuation growth rate, the electron temperature increase gives the higher fluctuation growth rate and the increasing ion temperature has the higher stabilization effect of drift wave. In GAMMA 10, during the potential formation by the P-ECH, the electron temperature goes up from 0.05 keV to about 0.10 keV, and ion temperature is kept at about 5 keV. The stabilization by the ion temperature effect is small. The electron density

profile is almost the same as that before and during P-ECH periods. During the periods without P-ECH, the negative electric fields have enhancement of diamagnetic drift. During the periods with P-ECH, the positive electric fields suppress the diamagnetic drift. The fluctuation suppressions by the higher potentials and positive electric fields are clearly observed.

4. Particle Flux Analysis

The particle flux was evaluated from the fluctuations of the potential and the density and their phase difference measured by GNPB. In GAMMA 10, the azimuthally propagating electrostatic fluctuations are observed. Radial particle flux estimated from the observed value is derived as

$$\Gamma_p \approx \frac{2}{B_0} \int_0^\infty k_\theta |\gamma_{n\phi}| \tilde{n} \tilde{\phi} \sin \alpha_{n\phi} d\omega, \quad (1)$$

where k_θ , $\gamma_{n\phi}$, \tilde{n} , $\tilde{\phi}$ and $\alpha_{n\phi}$ represent the wave number, the coherence between the density and the potential fluctuations, the density and the potential fluctuations, and the phase difference between the density and the potential fluctuations, respectively. The B- and P-ECH were applied from 150 to 190 ms and 155 to 175 ms, respectively, in order to produce the axial confining potential. We observed the frequencies of about 8 to 12 kHz in the potential and density fluctuations which correspond to the drift-type fluctuations. Figure 8 shows the temporal evolution of the diamagnetism (dotted line) and the observed radial particle flux related value obtained by the potential and density fluctuations at $R \sim 6$ cm (solid line). A good correlation between the diamagnetism and particle flux related value is obtained from eq. (1). The particle flux related value increase was observed in the diamagnetism decreasing phase. Moreover, the particle flux related value decrease with the increase in diamagnetism. During the periods from 150 to 155 ms, the large particle flux related value was observed, which was caused by B-ECH. In Fig. 9, we show the radial particle flux related value without (closed circles) and with P-ECH periods (open squares). The particle flux related values increase at the edge region during the period without P-ECH. These tell us one of the source of the anomalous radial transport is the potential and density fluctuations and the fluctuations decrease the plasma stored energy. Figure 9 shows that

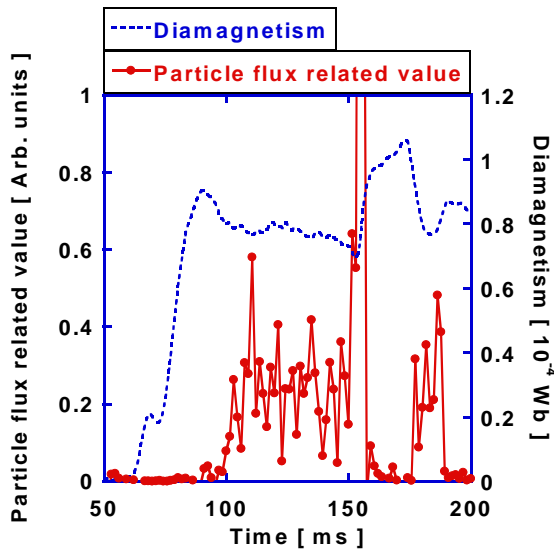


FIG. 8. Particle flux related value and diamagnetism.

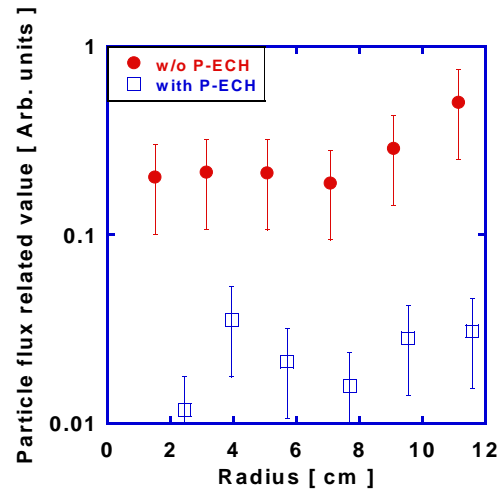


FIG. 9. the radial particle flux related value without (closed circles) and with P-ECH periods (open squares).

suppression of particle flux also reduced the radial particle flux with application of P-ECH and the stored energy quickly increased. Then the potential formation with application of P-ECH is the one of the key to control the plasma transport.

5. Summary

We studied the suppression of the density and potential fluctuations by applying P-ECH in the tandem mirror GAMMA 10. The higher potential and positive electric field formation in the central cell stabilizes the drift-type fluctuations. The correlation between the radial particle flux related value deduced from the phase differences of the density and potential fluctuations and stored energy is also studied by using GNPB. It is found that the radial anomalous transport induced by the drift-type fluctuations causes the reduction of the plasma stored energy. These results indicate the possibility of the suppression of the anomalous transport by the radial potential profile change with P-ECH. It suggests that the radial potential profile control is also useful to improve the radial plasma confinement in magnetic confinement devices.

Acknowledgments

The authors would like to thank members of GAMMA 10 group of the University of Tsukuba for their collaboration. This work was partly supported by Ministry of Education, Culture, Sports, Science and Technology, Grant-in-Aid for Scientific Research in Priority Areas, No 16082203 and NIFS collaboration research program, No NIFS04KUGM009.

References

- [1] A. Mase, et al., "Ambipolar potential effect on a drift-wave mode in a tandem-mirror plasma", *Phys. Rev. Lett.* **64** (1990) 2281-2884.
- [2] A. Mase, et al., "Measurement of dispersion-relation of waves in a tandem mirror plasma by the fraunhofer-diffraction method", *Rev. Sci. Instrum.* **61** (1990) 1247-1250.
- [3] A. Mase, et al., "Control of the radial electric-field and of turbulent fluctuations in a tandem mirror plasma", *Nuclear Fusion* **31** (1991) 1725-1733.
- [4] Y. Miyata, et al., "Observation of the effects of radially sheared electric fields by the use of a gold neutral beam probe", *Plasma Fusion Res.* **2** (2007) S1101.
- [5] M. Yoshikawa, et al., "Electron density fluctuation measurements using a multichannel microwave interferometer in GAMMA 10", *Rev. Sci. Instrum.* **77** (2006) 10E906.
- [6] M. Yoshikawa, et al., "Density fluctuation measurement for studying the effect of potential and electric field formation in GAMMA 10", *Plasma Fusion Res.* **2** (2007) 048.
- [7] H. Sanuki, "Stability of electrostatic drift waves in bumpy tori", *Phys. Fluids* **27**, (1984) 2500-2510.
- [8] MB. Chaudhry, et al., "Effects of an ambipolar field on stability of electrostatic drift waves in sheet plasmas", *J. Phys. Soc. Jpn.* **57**, (1988) 3043-3051.
- [9] R. Hatakeyama, et al., "Effects of controlled flow velocity shear in open-ended magnetized plasmas", *J. Plasma Fusion, Res.* **80** (2004) 299-305, in Japanese.
- [10] M. Yoshinuma, et al., "Control of radial potential profile and related low-frequency fluctuations in an ECR-produced plasma", *Phys. Lett. A* **254** (1999) 301-306.
- [11] M. Yoshinuma, et al., "Stabilization of low-frequency fluctuations by radial potential-profile control in an ECR-produced plasma", *Tran. Fusion Technol.* **35** (1999) 278-282.
- [12] P. A. Bagryansky, et al., "Influence of radial electric field on high-beta plasma

- confinement in the gas dynamic trap", *Trans. Fusion Sci. Technol.* **51** (2007) 340-342.
- [13] M. Yoshikawa, et al., "Use of a gold neutral beam probe to study fluctuation suppression during potential formation in the GAMMA 10 tandem mirror", *Fusion. Sci. Technol.* **57** (2010) 312-319.